*J. exp. Biol.* **102**, 13–23, 1983



# ELECTROPHYSIOLOGICAL AND MORPHOLOGICAL IDENTIFICATION OF ACTION POTENTIAL GENERATING SECRETORY CELL TYPES ISOLATED FROM THE SALIVARY GLAND OF *ARIOLIMAX*

BY JAMES M. GOLDRING*, JOANNE W. KATER AND STANLEY B. KATER

*Department of Zoology, University of Iowa, Iowa City, Iowa 52242*

(*Received 6 April 1982—Accepted 11 August 1982*)

SUMMARY

The salivary glands of the terrestrial slug, *Ariolimax*, are composed of several morphologically distinct cell types which are observable in thin pieces of living glands and in sectioned tissue viewed with the light or electron microscope. 'Blind' penetration via microelectrode into the gland reveals different classes of electrical activity including: (1) cells with fast action potentials; (2) cells with slow action potentials; and (3) cells with large resting potentials but which display only delayed rectification. After isolation of cells by enzymatic dissociation we could electrophysiologically characterize individual cell types and relate these to cell types identified morphologically in the living gland and under the light and electron microscopes. Microelectrode recordings from identified cell types have demonstrated: (1) the large granule cell type (granule diameter = 8–12 $\mu$m) displays a characteristic long duration, slow rise time action potential whose inward current is primarily carried by $Ca^{2+}$; (2) the medium granule cell type (granule diameter = 3–6 $\mu$m) displays only delayed rectification and (3) the small granule cell type (granule diameter = 1–2 $\mu$m) displays fast rise time, short duration action potentials whose inward current is also carried primarily by $Ca^{2+}$ ions.

The finding that morphologically distinct cell types display distinct electrical activity may indicate that different secretory products are released only under a specific set of conditions associated with changes in membrane potential.

## INTRODUCTION

The electrophysiology of exocrine secretory cells has received increasing attention over the last decade (see reviews by Peterson, 1976, 1980; and House, 1980). One of the goals of these studies has been to elucidate the relationship between electrical characteristics and the process of secretion. In the exocrine secretory cells of molluscs, regenerative electrical activity has been shown by research at this laboratory (Kater, 1977; Kater, Murphy & Rued, 1978; Kater, Rued & Murphy, 1978; Hadley, Murphy

*Present address: Department of Physiology, University of North Carolina Medical School, Chapel Hill, North Carolina 27514.

Key words: Salivary gland, electrophysiology, secretion.

& Kater, 1980). Stimulus–secretion coupling in these exocrine cells may thus be mechanistically similar to that found at the neuromuscular junction and the squid giant synapse. There are, however, potential pitfalls in this interpretation, since exocrine tissues are composed of cells which may communicate electrically with one another via low resistance junctions (e.g., Kater, Rued & Murphy, 1978; Kater & Galvin, 1978). The situation is further complicated when there are morphologically distinct secretory and nonsecretory cell types composing such an organ system (e.g., Boer, Wendelaar Bonga & van Rooyen, 1967; Walker, 1970; Beltz & Gelperin, 1979; Kater, Rued & Murphy, 1978). Thus, the electrical activity recorded from a gland cell may reflect the membrane properties of a closely communicating, yet morphologically different, neighbouring cell. In such a situation, the electrical activity of the cells can only be studied by recording from identified cells that have been isolated from one another. In the present investigation we have found that at least three different types of electrical activity can be recorded from the intact salivary gland of the slug.

## MATERIALS AND METHODS

*Ariolimax* were provided by Mr Robert Daub of Coos Bay, Oregon and could be maintained in our laboratory for 5–6 months. The slugs were kept at 13 °C in plastic boxes lined with moist paper towels and were fed zucchini and lettuce.

### *Dissection*

To remove the salivary gland the slug was first pinned, dorsal surface up, through the head and tail to a wax-covered dish. An incision was made along the dorsal midline from tail to head and the flaps retracted laterally. The gland, located just posterior to the buccal mass, is easily removed after cutting attachments to the underlying tissue and oesophagus, and the ducts to the buccal mass. The gland was stored in $Ca^{2+}$-free, high $Mg^{2+}$ saline (see Table 1) in the refrigerator for up to 48 h.

### *Cell isolation procedures*

A small piece of whole gland was minced with a razor blade in a few drops of $Ca^{2+}$-free, $Mg^{2+}$-free saline and was digested in 3 ml of 1·0 % collagenase (Sigma, Type I) at 30 °C in $Ca^{2+}$-free, $Mg^{2+}$-free saline in a shaker bath for 10–20 min. The precise duration was determined by visual inspection of samples. At the end of the digestion period the suspension was centrifuged at 50 ***g*** for 5 min. After aspirating the supernatant, the cell pellet was suspended in 3 ml of $Ca^{2+}$-free, $Mg^{2+}$-free saline containing 2 mM-EDTA and incubated for 10–20 min in a shaker bath at room temperature. This suspension was centrifuged at 50 ***g*** for 5 min and the pellet then suspended in 3 ml of normal saline (Table 1).

The above procedure was the most successful of many variations tried, including the use of trypsin, hyaluronidase and various combinations of these enzymes with collagenase. Digestion was carried out at 30 °C because the electrophysiological results suggested that higher temperatures damaged the tissue. Best results were obtained when the enzyme solution was prepared just prior to use. Since the cells adhere to glass, cell yields were increased by using only plastic vessels.

### *Electrophysiological methods*

*Intact gland*

A small piece of gland was stretched and pinned to a black Sylgard (Dow Corning) block which was then fitted into a Lucite chamber (Kater, Rued & Murphy, 1978) and was continuously perfused with saline solutions. In some cases, the tissue was first soaked in 0·2 % collagenase at 30 °C for 10–15 min; this seemed to aid penetration of the cells without noticeably affecting their electrical properties. Solutions could be changed rapidly, allowing manipulation of the ionic composition of the media. The time-course for a solution change was indicated by the time required to abolish the action potential in $Na^+$-free, $Ca^{2+}$-free media. This could be as little as 30 s for surface cells or up to 3 min for deeper cells. One to two additional minutes were then allowed before recordings were made.

Cells were impaled with microelectrodes filled with 3 M-potassium chloride or 4 M-potassium acetate. Intracellular recording and stimulation were accomplished by conventional techniques (Kater, Rued & Murphy, 1978). Current traces in Figs 2–6 are used to indicate only the time course of current injection and relative magnitude in any given series.

*Isolated cells*

Cells were deposited on coverslips coated with polylysine to promote adhesion. Coverslips were prepared by soaking them in a solution of poly-L-lysine (Sigma Type VII-B) in distilled water (2 mg/ml) for 18–24 h, washing in distilled water for 1 h and air drying. The coverslip was placed in a chamber whose bottom was also a glass coverslip since the cells were to be viewed from below on an inverted compound microscope (Zeiss, ICM) equipped with Nomarski optics.

Cells adhering to the coverslip were impaled with 3 M-potassium acetate-filled glass microelectrodes (d.c. resistance = 30–60 MΩ) bent within a few millimetres of their tips to facilitate movements within the condenser working distance. Recording and stimulation through individual microelectrodes were made by use of a high input impedance electrometer with integral current monitor (Dagan, Preamp-clamp). Signals were displayed on a Tektronix oscilloscope.

The cells were continuously perfused with saline by a Buchler Poly-staltic pump running at approximately 1 ml/min. Solutions were drawn off by a second channel of the same pump.

*Solutions*

The composition of the various solutions used is shown in Table 1.

### *Light and electron microscopy*

*Intact gland*

Tissue was fixed for 6 h at 4 °C in a modified Karnovsky's fixative (Karnovsky, 1965), containing 1 % paraformaldehyde and 3 % glutaraldehyde in 0·06 M-cacodylate buffer (pH 7·4) and postfixed in 1 % $OsO_4$ in cacodylate buffer. After dehydration

Table 1. *Bathing solutions (pH 7·7)*

| | NaCl | KCl | $CaCl_2$ | $MgCl_2$ | Tris*–HCl |
|---|---|---|---|---|---|
| | | | mmol/l | | |
| Normal saline | 80 | 4 | 7 | 5 | 5 |
| $Na^+$–free, $Ca^{2+}$–free saline | 0 | 4 | 0 | 12 | 94 |
| $Na^+$–free saline | 0 | 4 | 7 | 5 | 94 |
| $Ca^{2+}$–free saline | 80 | 4 | 0 | 12 | 5 |
| $Ca^{2+}$–free, high $Mg^{2+}$ saline | 68 | 4 | 0 | 20 | 5 |
| $Ca^{2+}$–free, $Mg^{2+}$–free | 98 | 4 | 0 | 0 | 5 |

* Tris = tris hydroxymethylaminomethane

in an ethanol series and embedding in Spurr's medium (Spurr, 1969), sections were cut with glass knives on a Porter Blum MT2 ultramicrotome. Thin sections were stained with 3 % aqueous uranyl acetate and with lead citrate (Venable & Coggeshall, 1965) and were viewed and photographed with a Phillips EM 300 electron microscope. Semi-thin sections (0·5 μm) were mounted unstained on glass slides and photographed with phase contrast optics on a Zeiss Photomicroscope.

*Isolated cells*

Dissociated cells, suspended in a drop of saline, were deposited on polylysine-coated coverslips (notched in one corner to serve as a landmark in subsequent processing) and left undisturbed in small Petri dishes for 20 min to allow cells to settle and adhere. Glutaraldehyde fixative (1 % in 0·05 M-cacodylate buffer, pH 7·2) was then applied dropwise to fill the dish, and cells were fixed for 1 h at 4 °C. After a buffer rinse the coverslips were inverted onto a drop of saline on a glass slide for viewing and photography on a Zeiss Universal Microscope equipped with a calibrated mechanical stage, Nomarski optics, and set up for Polaroid Type 105 photography. When an area of interest was located, its stage coordinates were recorded along with the coordinates of a landmark such as the notch, and the area was photographed at low power. This Polaroid print then served as a map of the area, allowing single cells to be numbered and photographed at higher power. The coverslip, removed from the slide, was then placed, cell-side up, in a Petri dish and was carried through osmification, alcohol dehydration and infiltration. Beem capsules were filled with Spurr's embedding medium so that there was a positive meniscus, and the coverslips were inverted onto this. After polymerization the approximate location of the cells of interest could be measured relative to the notch using the recorded coordinates. A dissecting microscope with magnification to 60× allowed exact localization of the cells by comparison with the Polaroid map. Marks whose extensions would intersect at the cell's location were made on the block itself and the coverslip was removed after spraying with a quick-freezing aerosol (Cryokwik). After trimming, the boundaries of the block face were drawn on the Polaroid map to allow easy identification of sectioned cells at the microscope.

Semi-thin and thin sections were cut, stained and photographed as described

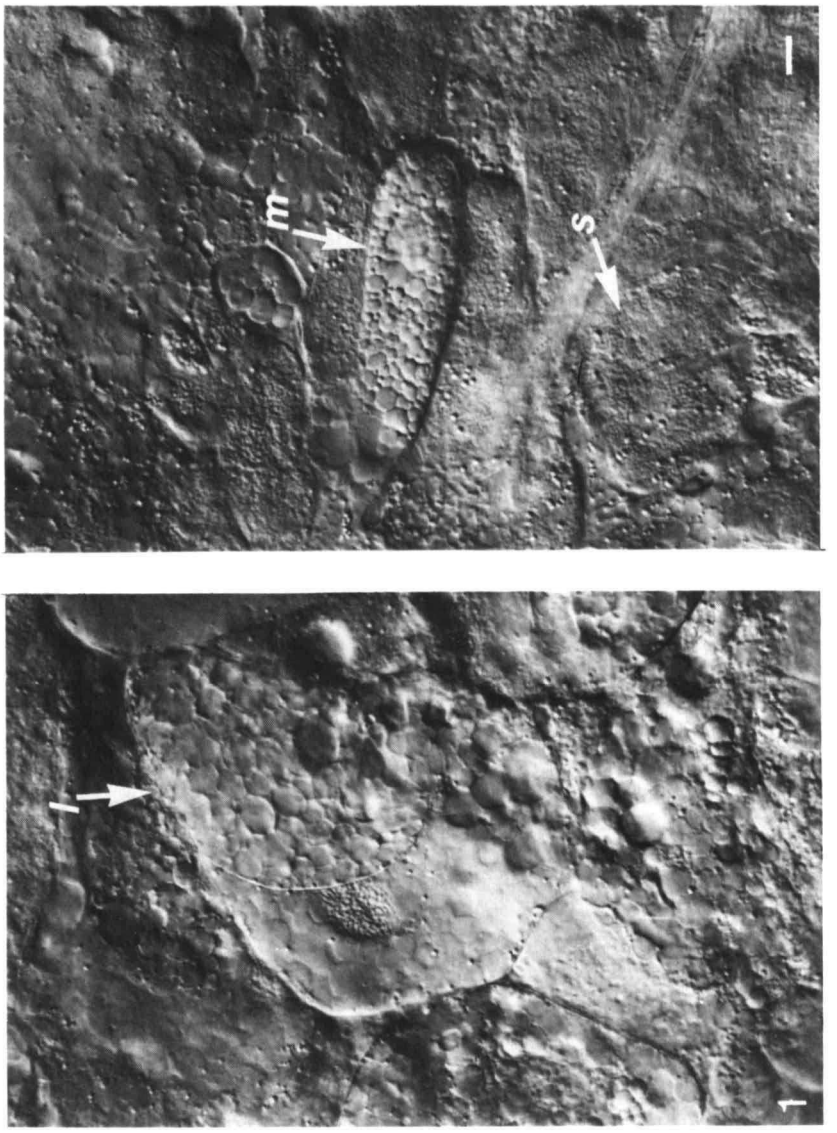


Fig. 1. Nomarski photomicrograph of gland cells in a thin piece of living gland. At least three different cell types can be readily recognized on the basis of granule size: *l*, large; *m*, medium; and *s*, small granule cell types. Bar, 10 $\mu$m.

above, with the exception that thin sections were mounted on formvar-coated, slotted grids.

## RESULTS

### *Appearance of gland under Nomarski optics*

The transparency of the living gland allows ready visualization with Nomarski optics of many focal planes through a thin piece of tissue. Apparent secretory activity and passage of material through a duct system can be observed clearly in such preparations. The living gland consists of a variety of morphologically distinct cell types (Fig. 1). While the total number of cell types is as yet unknown, three were readily defined on the basis of the appearance and size of their secretory granules: (1) small granule (1–2 $\mu$m granule diameter, which at 40× magnification have a rough-textured appearance, but individual granules are not generally resolved); (2) medium granule (3–6 $\mu$m granule diameter); and (3) large granule (8–12 $\mu$m granule diameter) cell types (Fig. 1). Cell size also varies with cell type; large granule cells can exceed 100 $\mu$m in at least one dimension, while small and medium granule cells are considerably smaller (although some in both classes reach 85 $\mu$m in diameter).

### *Electrophysiology of intact gland*

Cells impaled by blind penetration into the gland displayed three classes of electrical activity. In response to depolarizing current injection many cells were electrically inexcitable. These cells often had large resting potentials, and thus did not appear to be damaged. Other cells generated overshooting, all-or-none action potentials. These action potentials were of two classes (Fig. 2), being distinguished primarily on the basis of their duration and the presence of a plateau on the falling phase of the slower action potential. In some cells, depolarizing current pulses elicited graded responses, but it was not possible to determine if the response was of a third distinct class or the result of impalement injury. The ionic basis of the more frequently encountered fast action potential was investigated to serve as a basis for later comparison with enzymatically isolated cells (Fig. 3). When $Na^+$ and $Ca^{2+}$ were removed from the bathing medium and replaced with Tris and $Mg^{2+}$ respectively, the action potential was abolished. If $Ca^{2+}$, but not $Na^+$, was added back to the perfusion solution, the action potential was restored, although its amplitude was somewhat smaller. On the other hand, if $Na^+$, but not $Ca^{2+}$, was returned to the bathing medium, only a small regenerative response was elicited by depolarizing current pulses. In other preparations, where $Ca^{2+}$ carries current during the action potential, $Co^{2+}$ ions have been shown to be an effective blocker of $Ca^{2+}$ currents (Geduldig & Junge, 1968; Hagiwara & Takahashi, 1967). The addition of 10 mM-$CoCl_2$ to normal saline (both $Na^+$ and $Ca^{2+}$ present) greatly reduced the amplitude of the action potential (Fig. 3). Taken together, these data suggest that during the rising phase of the action potential $Ca^{2+}$ ions are the predominant current carriers in this cell type.

In order to correlate directly the electrical activity of a particular cell type with its morphology, further electrophysiological experiments were performed on single cells isolated from the salivary gland by enzymatic dissociation. This provided a degree of

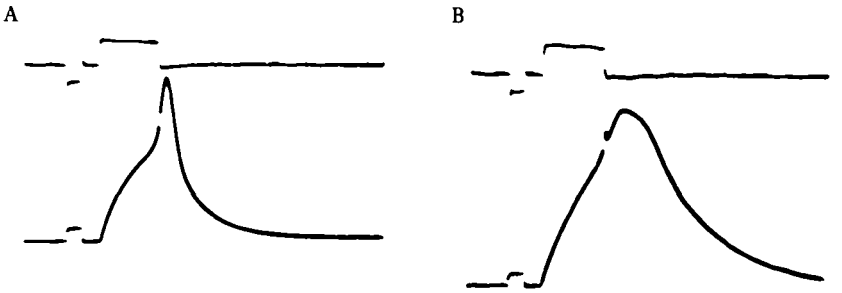


Fig. 2. Intracellular microelectrode recordings from cells in the intact gland. Cells were impaled blindly as described in the text. Two distinct types of action potentials were observed in response to intracellularly injected current: the fast rising, short duration spike (A) and a more slowly rising, long duration spike shown in B. Top trace is a current monitor record. Bottom trace is the voltage record. The calibration pulse at the beginning of the voltage trace is 10 mV and 10 ms.

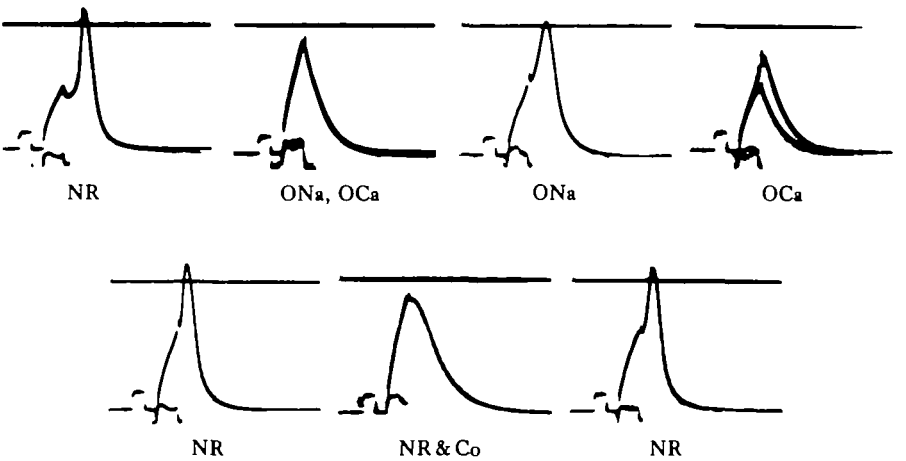


Fig. 3. Effect of changing the ionic composition of the perfusion solution on the action potential of a cell in the intact gland. The action potential as seen in normal Ringer (NR) is completely abolished in $Ca^{2+}$-free, $Na^{+}$-free (ONa, OCa) saline. An overshooting spike is present when $Na^{+}$ alone is removed from the media (ONa), but only a small regenerative response remains when $Ca^{2+}$ alone is removed (OCa). Another series on the same cell shows that addition of 10 mM-$CoCl_2$ to normal saline (NR & Co) abolishes all but a small regenerative response. This effect is readily reversible (NR, right). Top trace in each record is the zero potential level and the lower trace is the intracellular potential level. The calibration pulse at the beginning of the voltage record is 10 mV and 10 ms.

resolution not obtainable in the intact gland since it is not possible to discern the morphology of cells in the whole gland with the optical configuration required for electrophysiology.

### *Studies of isolated cells*

In preparations of dissociated cells, three predominant cell types were clearly distinguished (Fig. 4). No attempt was made to determine the viability or yield of the preparation quantitatively. However, based on casual inspection, approximately 30 % of the cells were viable (as judged from the correlation of the microscopic appearance with subsequent electrophysiological experiments). This relatively low yield of cells posed no problems in the present study since bulk properties of the cell suspension were

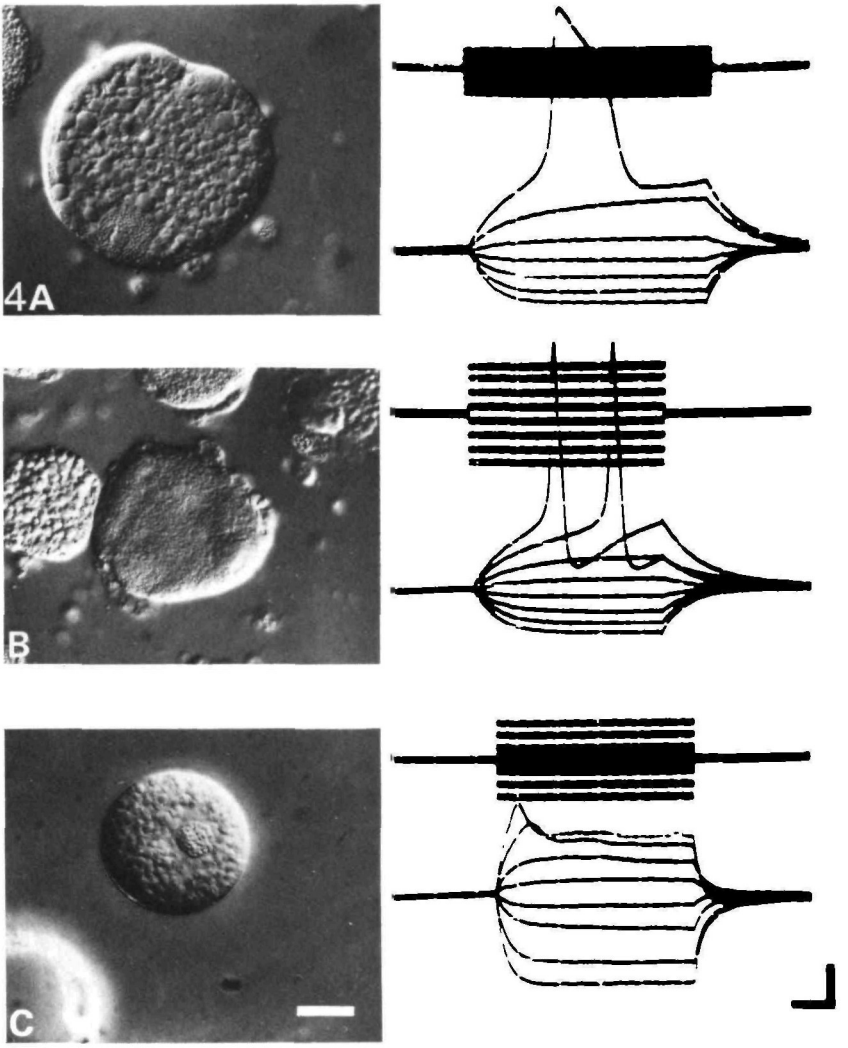


Fig. 4. Nomarski photomicrographs of representative dissociated cells opposite the type of activity such a cell displays. Large (A), small (B) and medium (C) granule cells are shown (bar = 20 μm). Current was passed through the recording microelectrode via a bridge circuit. Both large and small granule cells generate overshooting, all-or-none action potentials in response to depolarizing current pulses (A and B); only delayed rectification is evident in medium granule cells in response to large depolarizing pulses (C). The top trace in each record is the zero potential level and current monitor output; the lower trace is the membrane potential record. The calibration (lower right) is 20 mV and 50 ms.

not studied and one could readily select viable cells for electrophysiological study. Among the cell types observed with Nomarski optics were three types that were similar to those observed in the intact gland, with large, small and medium granules (Fig. 4). The largest of the large granule cells apparently do not survive dissociation. While these too might be isolated in viable condition with a more refined dissociation protocol, our simplified procedure was adequate for our purposes, yielding cells of 80 $\mu$m or greater.

Isolated gland cells were studied by impaling cells with a single microelectrode for passing current and recording membrane potential. Both large and small granule cells gave overshooting action potentials in response to depolarization (Fig. 4A, B) while the medium granule cell was electrically inexcitable and displayed only delayed rectification (Fig. 4C). The two types of action potentials resembled those observed in the intact gland; the spike of the large granule cell was longer in duration than the spike of the small granule cell, and the large granule cell spike had a plateau on the falling phase. Membrane potential, input resistance and spike overshoot were measured in a number of large and small granule cells (Table 2). Small granule cells had an average resting potential of 73 mV, an average input resistance of 158 M$\Omega$ and an average spike overshoot of 29 mV. Large granule cells had an average resting potential of 60 mV, an average input resistance of 306 M$\Omega$ and an average spike overshoot of 38 mV. The values of input resistance are quite high in relation to the large size of the cells. Some large and small granule cells did not generate spikes at the end of the stimulus pulse; however, the input resistance of these cells was low and it was assumed they were damaged. No data were taken from such cells.

The ionic basis of the rising phase of the action potential was investigated in both small (Fig. 5) and large (Fig. 6) granule cells. When both $Na^+$ and $Ca^{2+}$ were removed from the bathing medium, small granule cells were incapable of generating an action potential (not shown). If $Na^+$, but not $Ca^{2+}$, were present only a small response could be elicited by the stimulus pulse (OCa, Fig. 5A). However, when $Ca^{2+}$, but not $Na^+$, was present the cell could still generate an overshooting spike (ONa, Fig. 5A). When 10 mM-$CoCl_2$ was added to normal saline solution, the amplitude of the spike was greatly reduced (NR & Co, Fig. 5B). Responses of the large granule cells to similar changes of the bathing medium (Fig. 6) were similar to those of the small granule cells. The only difference noted was that the large granule cells displayed no regenerative activity when the cell was bathed in a $Ca^{2+}$-free medium. One puzzling finding was that addition of 10 mM-$Co^{2+}$ to normal saline did not completely abolish the response of the large granule cell to depolarization as evidenced by the non-exponential fall of potential at the end of the current pulse. This was a routine observation. These data suggest that $Ca^{2+}$ ions are the predominant current carrier during the action potential in both small and large granule cells. There appears to be a small $Na^+$ component to the spike of the small granule cells, but it is not certain whether $Na^+$ ions carry significant current during the spike of the large granule cell. Since the morphological appearance and spike characteristics of the isolated, small granule cell were similar to those observed in the intact gland, it appears that the isolation procedure has not significantly compromised the functional integrity of the cell.

Table 2. *Characteristics of large and small granule cells*

| | Resting potential | Input resistance | Overshoot |
|---|---|---|---|
| Small granule | 73 ± 6 mV (n = 16) (range 60–82 mV) | 158 ± 98 MΩ (n = 17) (range 50–450 MΩ) | (29 ± 7 mV (n = 13) (range 20–42 mV) |
| Large granule | 60 ± 10 mV (n = 11) (range 42–80 mV) | 306 ± 104 MΩ (n = 22) (range 167–550 MΩ) | 38 ± 4 mV (n = 11) (range 28–44 mV) |

*Morphology of action potential generating cells*

Histological and ultrastructural observations were made on the spiking secretory cell types of the salivary gland in order to provide further data for cell type classification. Dissociated cells were identified under Nomarski optics as large (Fig. 7A) and small (Fig. 7C) granule cells. The *same* cells shown in Fig. 7A and C were then embedded and sectioned and are shown in the phase photomicrographs in Fig. 7B (large) and Fig. 7D (small). (These same cells were also thin sectioned and viewed with the electron microscope (not shown), and while identification of cell type was possible, the quality of preservation in these cells after the lengthy procedures of identification and photography was not adequate to provide ultrastructural details.) The morphology revealed by sectioning these isolated cells clearly corresponds to cell

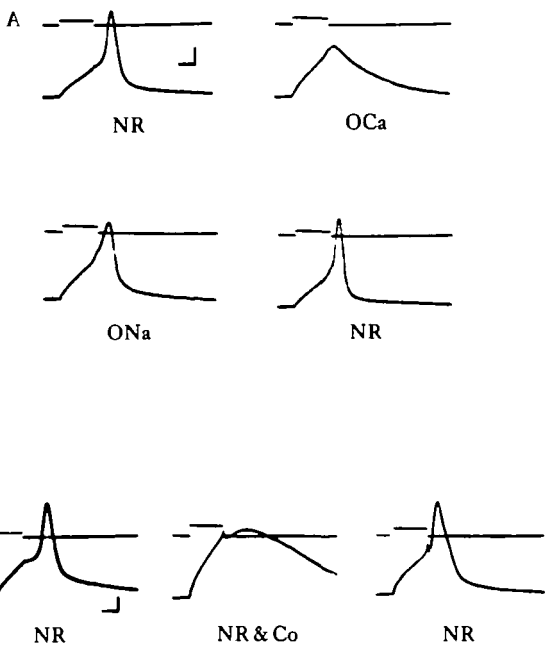


Fig. 5. The sequential effect of alterations of the bathing medium on the action potential in isolated, small granule cells. A. Action potential elicited in normal Ringer (NR). Regenerative activity is almost completely abolished in $Ca^{2+}$-free saline (OCa) but $Na^{+}$-free (ONa) saline causes only a slight reduction in action potential overshoot. B. A series in a second small granule cell shows that addition of 10 mM-$CoCl_2$ to normal saline (NR & Co) causes a reversible reduction of spike amplitude. Calibration in A and B: 20 mV and 20 ms. The top trace in each record is zero potential level and current monitor output; lower trace is intracellular potential record.

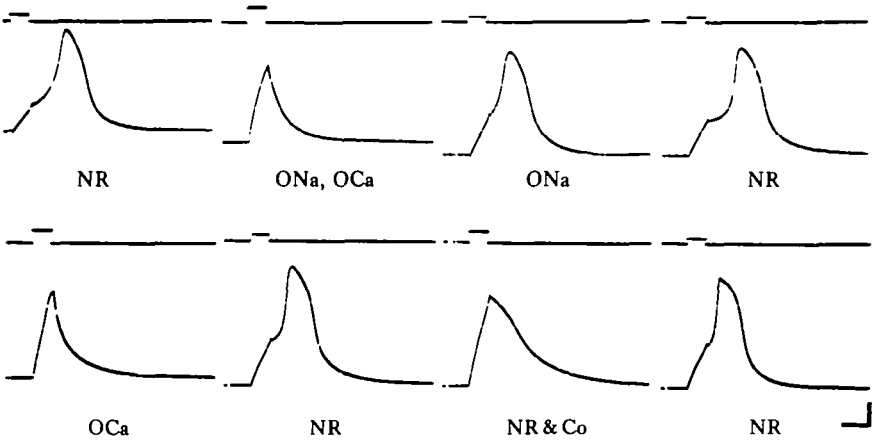


Fig. 6. The effect of alterations of the bathing medium on the action potential in an isolated, large granule cell. Action potential in normal Ringer (NR) is completely abolished in $Ca^{2+}$-free, $Na^{+}$-free medium (ONa, OCa). The action potential was present in $Na^{+}$-free media (ONa) but was abolished in $Ca^{+2}$-free media (OCa). Addition of 10 mM-$CoCl_2$ to normal saline (NR & Co) reduced the amplitude of the spike, which then recovered after $Co^{2+}$ was washed out. All records from the same cell. The top trace is the current monitor output (does not indicate zero potential); the lower trace is the membrane potential record. Calibration: 20 mV and 20 ms.

types seen in sections of the whole gland (Fig. 7E, F). Here adjacent semi-thin (Fig. 7E) and thin (Fig. 7F) sections allow the same cells to be viewed with both the light and electron microscope.

The large granule cell (Fig. 7A, B, E, F) is characterized by the density and large size of its granules (up to 10 $\mu$m diameter) and the large cell size, which can exceed 100 $\mu$m in length (some shrinkage in processing is unavoidable and measurements of processed cells and granules are not as large as those of living cells). The small granule cell (Fig. 7C, D, E, F) is smaller in size ($\simeq$35 $\mu$m in diameter) and contains small (1–2 $\mu$m), electron-lucent granules with characteristic intragranular densities. These two cell types are easily identifiable under Nomarski optics prior to intracellular recordings and can be linked reliably to the corresponding dense large granule cell type and small granule cell type seen in plastic sections of these glands. The medium granule cell has not been carried through this rigorous identification procedure and so cannot yet be linked with certainty to a cell type seen in sectioned material.

## DISCUSSION

The action potential of both large and small granule salivary gland cells was shown here to be primarily $Ca^{2+}$-dependent, as with the ionic basis of the action potential described in the whole gland of *Helisoma* (Hadley *et al.* 1980). Spike activity also has previously been reported in the pedal gland of the slug (Kater, 1977) and this has been shown to be dependent both on $Na^{+}$ and $Ca^{2+}$. Although action potentials have not been observed in mammalian salivary glands (Kater & Galvin, 1978) they have been observed in isolated mammalian adrenal medullary cells (Biales, Dichter & Tischler, 1976; Brandt, Hagiwara, Kidokoro & Miyazaki, 1976); the spike here is primarily $Na^{+}$-dependent although a small $Ca^{2+}$ component can be observed under appropriate

conditions (Biales *et al.* 1976). Pancreatic islet cells show slow depolarizing waves with superimposed spikes in response to applied glucose (Dean & Matthews, 1970; Matthews & Sakamoto, 1975; Meissner & Schmelz, 1974); both the depolarizing wave and spike are $Ca^{2+}$-dependent.

It is important to recognize that the individual cell types, which make up any glandular system, normally function as an integrated ensemble (for *Helisoma* see Kater, Murphy & Rued, 1978 and Senseman & Salzburg, 1980). The present communication, however, speaks only to the individual properties of particular cell types rather than attempting to ask about interrelationships. Such interactions deserve investigation in their own right. This fact notwithstanding, it is clear that the kind of information obtained by partitioning the complexity of this glandular tissue may be masked in studies which rely on data solely from intact glands. The finding that morphologically distinct cell types display different electrical activity may indicate that different secretory products are released only under a specific set of conditions associated with changes in membrane potential.

The purpose of the morphological studies described here is to establish a method of reliable classification of isolated cells and not to provide an ultrastructural analysis of these cells such as has been done on pancreatic acinar cells (Amsterdam & Jamieson, 1974) and adrenal medullary cells (Fenwick, Fajdiga, Howe & Livett, 1978). While the quality of the preservation of our material is certainly adequate for our present purposes, it is lower than that obtained in fixing a freshly dissociated cell pellet. A thorough ultrastructural and histochemical analysis is presently in progress (J. W. Kater, R. G. Kessel, S. B. Kater and J. G. Assouline, in preparation). These studies indicate not only that different cell types are present in this gland but that the secretory products elaborated by these cell types are also histochemically different.

Advantages of working with dispersed single cells have been apparent since Douglas' early work on the mast cell (Kanno, Cochrane & Douglas, 1973). With great technical skill Douglas and coworkers were able to employ these small cells for direct visual observation of exocytosis. An important feature of the molluscan cells in the present study is the fact that a single granule in the large granule cell type can be 10 $\mu$m in diameter, i.e., as large as an entire mast cell. We have made preliminary observations of exocytosis in these living cells during microelectrode penetration in order to assess the feasibility of examining the problem of stimulus–secretion coupling (Llinas & Heuser, 1977). Under appropriate stimulus and cinematographic conditions the secretory event might be directly observed in these living exocrine cells under direct voltage control, thus providing an opportunity to study the relationship of such important parameters as Vm, $\Delta Ca^{2+}{}_{in}$ and exocytosis in a single system.

Fig. 7. Nomarski photomicrographs of isolated large (A) and small (C) granule cells. B and D are phase photomicrographs of the same cells after embedding and sectioning. The morphology revealed by sectioning these dissociated, classified cells clearly corresponds to two cell types seen in the sectioned gland (*l*, large and *s*, small granule cell types in E and F). E is a phase photomicrograph of a semi-thin section. F is an electron micrograph from a thin section cut adjacent to the section shown in E. The asterisks in E and F mark identical areas in each section and extend the morphological data on action potential generating cells to the ultrastructural level. Bars: A–D, 10 $\mu$m; E, 10 $\mu$m; F, 1 $\mu$m.

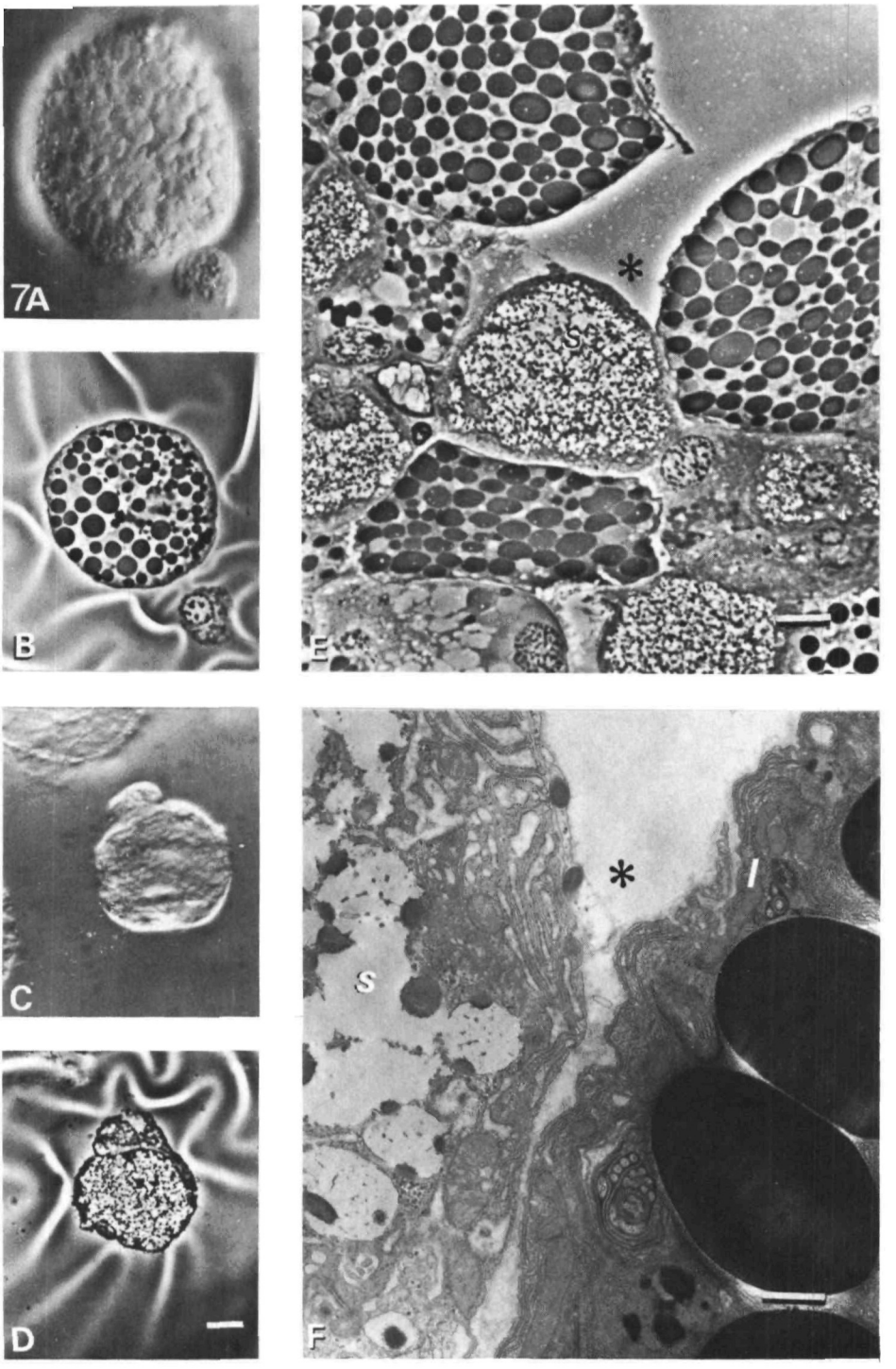
7A
B
C
D
E
F
S
I
*

We thank Robert Hadley and Drs A. D. Murphy and Brian Salzberg for their critical reading of this manuscript and F. Hunter, M. Jolly and P. Gade for assistance in its preparation. This research was supported by NIH grant 5 RO1 AM19858 to S. B. Kater and NIH fellowship 1 F32 NS05797 to J. M. Goldring.

## REFERENCES

AMSTERDAM, A. & JAMIESON, J. D. (1974). Studies on dispersed pancreatic exocrine cells. I. Dissociation technique and morphological characteristics of separated cells. *J. Cell Biol.* **63**, 1037–1056.

BELTZ, B. & GELPERIN, A. (1979). An ultrastructural analysis of the salivary system of the terrestrial mollusc, *Limax maximus*. *Tissue and Cell* **11**, 31–50.

BIALES, B., DICHTER, M. & TISCHLER, A. (1976). Electrical excitability of cultured adrenal chromaffin cell. *J. Physiol., Lond.* **262** 743–753.

BOER, H. H., WENDELAAR BONGA, S. E. & VAN ROOYEN, N. (1967). Light and electron microscopical investigations on the salivary glands of *Lymnaea stagnalis*. L. *Z. Zellforsch. mikrosk. Anat.* **76**, 228–247.

BRANDT, B. L., HAGIWARA, S., KIDOKORO, Y. & MIYAZAKI, S. (1976). Action potentials in the rat chromaffin cell and effects of acetylcholine. *J. Physiol., Lond.* **263**, 417–439.

DEAN, P. M. & MATTHEWS, E. K. (1970). Electrical activity in pancreatic islet cells: effect of ions. *J. Physiol., Lond.* **210**, 265–275.

FENWICK, E. M., FAJDIGA, P. B., HOWE, N. B. S. & LIVETT, B. G. (1978). Functional and morphological characterization of isolated bovine adrenal medullary cells. *J. Cell Biol.* **76**, 12–30.

GEDULDIG, D. & JUNGE, D. (1968). Sodium and calcium components of action potentials in the *Aplysia* giant neurone. *J. Physiol., Lond.* **199**, 347–365.

HADLEY, R. D., MURPHY, A. D. & KATER, S. B. (1980). Ionic bases of resting and action potentials in salivary gland acinar cells of the snail *Helisoma*. *J. exp. Biol.* **84**, 213–225.

HAGIWARA, S. & TAKAHASHI, K. (1967). Surface density of calcium ions and calcium spikes in the barnacle muscle fiber membrane. *J. gen. Physiol.* **50**, 583–601.

HOUSE, C. R. (1980). Physiology of invertebrate salivary glands. *Biol. Rev.* **55**, 417–473.

KANNO, T., COCHRANE, D. E. & DOUGLAS, W. W. (1973). Exocytosis (secretory granule extrusion) induced by injection of calcium into mast cells. *Can. J. Physiol. Pharm.* **51**, 1001–1004.

KARNOVSKY, M. J. (1965). A formaldehyde–glutaraldehyde fixative of high osmolality for use in electron microscopy. *J. Cell Biol.* **27**, 137A.

KATER, S. B. (1977). Calcium electroresponsiveness and its relationship to secretion in molluscan exocrine gland cells. In *Society for Neuroscience Symposia*, Vol. 2, (eds W. M. Cowan & J. A. Ferendelli), pp. 195–214. Society for Neuroscience. Bethesda, Md.

KATER, S. B. & GALVIN, N. J. (1978). Physiological and morphological evidence for coupling in mouse salivary gland acinar cells. *J. Cell. Biol.* **79**, 20–26.

KATER, S. B., MURPHY, A. D. & RUED, J. R. (1978). Control of the salivary glands of *Helisoma* by identified neurones. *J. exp. Biol.* **72**, 91–106.

KATER, S. B., RUED, J. R. & MURPHY, A. D. (1978). Propagation of action potentials through electrotonic junctions in the salivary glands of the pulmonate mollusc, *Helisoma trivolvis*. *J. exp. Biol.* **72**, 77–90.

LLINAS, R. R. & HEUSER, J. E. (1977). Depolarization-release coupling systems in neurons. *Neurosci Res. Program Bull.* **15**, No. 4.

MATTHEWS, E. K. & SAKAMOTO, Y. (1975). Electrical characteristics of pancreatic islet cells. *J. Physiol., Lond.* **246**, 421–437.

MEISSNER, H. P. & SCHMELZ, H. (1974). Membrane potential of beta-cells in pancreatic islets. *Pflügers Arch. ges. Physiol.* **351**, 195–206.

PETERSON, O. H. (1976). Electrophysiology of mammalian gland cells. *Physiol. Rev.* **56**, 535–577.

PETERSON, O. H. (1980). *The Electrophysiology of Gland Cells*. 253 pp. New York: Academic Press.

SENSEMAN, D. M. & SALZBERG, B. M. (1980). Electrical activity in an exocrine gland: optical recording with a potentiometric dye. *Science N.Y.* **208**, 1269–1271.

SPURR, A. R. (1969). A low viscosity epoxy resin embedding medium for electron microscopy. *J. ultrastruct. Res.* **26**, 31–43.

VENABLE, J. H. & COGGESHALL, R. (1965). A simplified lead citrate strain for use in electron microscopy. *J. Cell Biol.* **25**, 407.

WALKER, G. (1970). Light and electron microscope investigations on the salivary glands of the slug, *Agriolimax reticulatus* (Muller). *Protoplasma* **71**, 111–126.